Applied optical properties of diamond

E. I. Lipatov, D. E. Genin, D. V. Grigor'ev, V. F. Tarasenko, A. G. Burachenko, E. Kh. Baksht, and D. V. Beloplotov

View Online

Export Citation

ARTICLES YOU MAY BE INTERESTED IN

Luminescence of Ti:Al$_2$O$_3$-media induced by pinched "overaccelerated" electron-Ti-ion beams
AIP Conference Proceedings **2069**, 030007 (2019); https://doi.org/10.1063/1.5089843

Pyramids <001> and <011> in natural diamond
AIP Conference Proceedings **2069**, 040006 (2019); https://doi.org/10.1063/1.5089849

Perspective: Is there a hysteresis during reactive High Power Impulse Magnetron Sputtering (R-HiPIMS)?
Journal of Applied Physics **121**, 080901 (2017); https://doi.org/10.1063/1.4976717

Applied Optical Properties of Diamond

E. I. Lipatov[1, 2, a)], D. E. Genin[1], D. V. Grigor'ev[2], V. F. Tarasenko[1], A. G. Burachenko[1], E. Kh. Baksht[1] and D. V. Beloplotov[1]

[1]*Institute of High Current Electronics, Siberian Branch, Russian Academy of Sciences, 2/3, Akademichesky Avenue, 634055, Tomsk, Russia*
[2]*Tomsk State University, 36, Lenina Avenue, 634050, Tomsk, Russian Federation*

[a)]Corresponding author: lipatov@loi.hcei.tsc.ru

Abstract. In our paper we report about the optical properties of diamonds having applied sense. Radiation destruction manifests itself in the form of absorption bands and luminescence of vacancies and interstitials. The charge state of the NV centers depends on the impurity-defective composition of the sample. Accelerated particles lose their energy to Cherenkov radiation. The fine splitting of the free exciton state affects the absorption and luminescence spectra in the recombination bands of free excitons and their condensed state.

INTRODUCTION

Diamond-based detectors of ionizing radiation and UV photodetectors have been widely used for quite a long time [1,2]. The basis is the generation of charge carriers when a sample absorbs the energy of photons or particles, and the drift of non-equilibrium charge carriers in an external field. Recently, diamond began to be used to detect runaway electrons in toroidal magnetic plasma confinement installations of the TOKAMAK type using measurements of Cherenkov radiation (ChR) [3]. In this paper, we report on the ChR measurement in natural and synthetic diamond as a result of exposure to runaway electron beams with a duration of ~ 100 ps generated in a gas diode [4].

In the near future, it is quite possible to create diamond cathodoluminescent (CL) sources of ultraviolet (UV) radiation based on the radiative recombination of free excitons at 235 nm. Currently, LEDs on semiconductor compounds, quantum wells, etc. work effectively at wavelengths of more than 350 nm [5]. Therefore, diamond CL-UV sources can find their niche in the market [6]. In this regard, the diagnosis of radiation destruction of the diamond lattice remains an urgent task. Identifying the correlation of the impurity-defective composition of the sample and the intensities of absorption and luminescence bands caused by vacancies and interstitials has practical significance [7].

The development of high-power solid-state diamond switches would seem to have stopped due to a fundamental limitation – free excitons (FEs) do not participate in the drift. However, the relatively recent detection in diamond the FE condensation in droplets of an electron-hole liquid (EHL) at sufficiently high temperatures (up to 200 K) [8,9] gives a chance for the use of diamond in high-current electronics. EHL droplets have a surface charge, therefore, are involved in the drift. The speed of sound in diamond is high ~ $2 \cdot 10^6$ cm/s. This value is an order of magnitude less than the saturated velocity of the carriers in the diamond. Nevertheless, the obtained preliminary data indicate a significant enhancement of the photocurrent in diamond under the conditions of EHL existence [10].

The tasks of quantum computing create the need for lasers in the visible range on the basis of diamond [11]. The charge state of the NV defect in natural samples depends on the impurity-defect composition [12]. This paper presents data on the observation of the vibronic bands of the NV center in two charge states in the absorption and luminescence spectra of a natural sample subjected to radiation-thermal treatment.

This paper is a brief review of research on the applied optical properties of diamond conducted in the Laboratory of Optical Radiation of the Institute of High Current Electronics, Siberian Branch of the Russian Academy of

Sciences, Tomsk. I.e. those optical properties of diamonds that we need to study for further research and, potentially, to create devices based on diamond.

RADIATION DEFECTS IN THE OPTICAL SPECTRA OF DIAMOND

We had 4 samples at our disposal, irradiated by beams of electrons and neutrons with different doses and further annealing: natural – CN5, CN11 and synthetic, obtained at high pressures and high temperatures (HPHT) – CN8, CN12. Figure 1 (a) shows the absorption spectra for the HPHT samples when cooled with liquid nitrogen and at room temperature. Neither in the PL spectra nor in the CL spectra of all 4 samples, the vibronic GR1 system was not observed. GR1 system is characterized by a low luminescence decay time (0.5–2 ns) and a high probability of non-radiative relaxation processes [13].
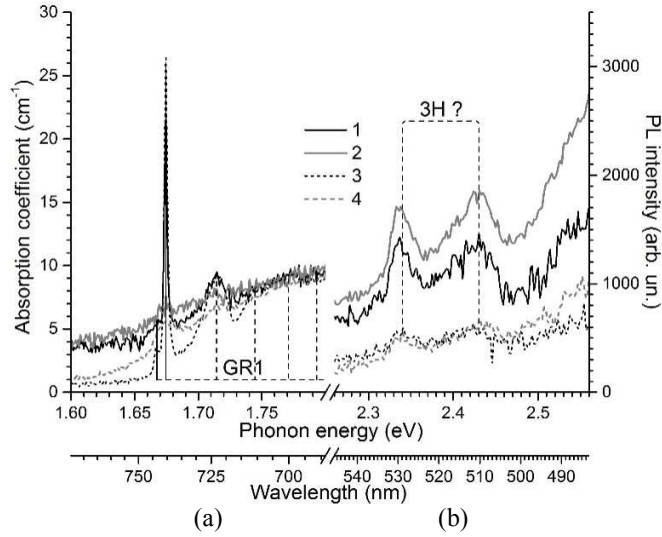
FIGURE 1. Radiation defects in the optical spectra of diamonds. a) Vibronic system GR1 of neutral vacancy in the absorption spectra of synthetic HPHT samples CN8 (curves 1 and 2) and CN12 (curves 3 and 4) when cooled with liquid nitrogen (curves 1 and 3) and at room temperature (curves 2 and 4). The ZPL doublet of GR1 is located at 1.673 and 1.665 eV (740.9 and 744.4 nm). b) Luminescence bands at 2.34 and 2.43 eV (530 and 510 nm) at room temperature in the photoluminescence spectra of pure CVD samples – polycrystalline C5 (curves 1 and 2) and single crystal C10 (curves 3 and 4) – when excited with excimer lamps at 206 nm (curves 1 and 3) and at 222 nm (curves 2 and 4). These bands were conditionally attributed to phonon replicas of the ZPL of system 3H at 2.462 eV (503.4 nm).

The vibronic system of a neutral vacancy shows itself in the optical absorption spectra in the form of a doublet of zero-phonon lines (ZPL) at 1.673 and 1.665 eV (740.9 and 744.4 nm) and a phonon wing in the long-wavelength area. The concentration of neutral vacancies can be estimated by the formula [12]:

$$N_{V^0} = 1.02 \cdot 10^{19} \cdot \int \alpha_{GR1} ,\qquad(1)$$

where $\int \alpha_{GR1}$ [eV/cm] – integral under the ZPL at 1.673 eV of GR1 when the sample is cooled with liquid nitrogen.

For the dominant ZPL at 1.673 eV (740.9 nm), the temperature dependences of the absorption coefficient in the range of 80–300 K are well approximated by the Mott law:

$$\alpha(T) = \frac{\alpha_0}{1 + A \cdot e^{-\Delta E / k_B T}} ,\qquad(2)$$

Where α_0 is the absorption coefficient at $T \to 0$ K, A is the quenching constant, ΔE is the quenching activation energy, k_B is the Boltzmann constant.

Table 1 shows the values of the absorption coefficient at 1.673 eV, the integral under the ZPL at 1.673 eV, the concentration of the neutral vacancy in the sample, and the values of α_0, A, and ΔE for each of the 4 samples. In the future, we plan to examine in details the correlation between the GR1 system and the impurity-defect composition of diamond samples, and establish a quantitative relationship.

TABLE 1. Values of the absorption coefficient in the dominant zero-phonon line of the neutral vacancy at 1.673 eV (740.9 nm) α_{GR1}, the integral under the zero-phonon line $\int\alpha_{GR1}$, the estimate of neutral vacancy concentration $N_V{}^o$, the value of the absorption α_0 at $T \rightarrow 0$, quenching constant according to Mott law A, activation energy of quenching ΔE for four diamond samples subjected to radiation destruction.

Sample	α_{GR1}, cm^{-1}	$\int\alpha_{GR1}$, eV/cm	$N_{V_o}\times10^{18}$, cm^{-3}	α_0, cm^{-1}	A	ΔE, meV
CN11	6.32	0.017	0.17	7.4	18.7	34.6
CN8	15.1	0.045	0.46	18.5	17.7	30.9
CN12	26.9	0.076	0.78	27.5	27.4	46.3
CN5	42.4	0.144	1.47	45.3	43.4	52.7

We found a photoluminescence (PL) band with peaks at 2.34 and 2.43 eV (530 and 510 nm) in high-purity CVD diamonds subjected to small doses of ionizing radiation (see Fig. 1 (b)). This band was also observed in the CL spectra when excited by beams with an electron maximum at ~ 80–100 keV.

The PL was excited at wavelengths of 172, 206, 222, 282, and 308 nm. When excited in the region of fundamental absorption, this band was observed. When excited by photons with an energy of less than the energy gap, this band was not observed.

After additional measurements, it will be possible to establish a level map. Due to the connection with the radiation damage and the spectral position of this band, we assume that we observed phonon replicas of ZPL at 2.462 eV (503.4 nm) of the 3H vibronic system [12]. The centers of the 3H band are their own interstitials.

CHARGE STATES OF THE NV DEFECT IN NATURAL DIAMOND

The natural sample CN4 was previously subjected to radiation-thermal treatment with unknown parameters. In the absorption spectra (see Fig. 2 (a)), this sample demonstrated intensive N3 systems (N_3V defect, 2.985 eV, 415 nm) and H3 (N_2V center, 2.463 eV, 503 nm), and weaker ZPL of the NV defect at zero (NV^0, 2.156 eV, 575 nm) and negative (NV^-, 1.945 eV, 638 nm, only when cooled) charge states. In addition, a wide band at 1.5 eV can be the N1 system – the forbidden transition of the N_3V defect [12].

In the cathodoluminescence spectra (80–100 keV, 2 ns), intense systems N3, N3a (N_3V-$(C_i)_n$-defect, 2.68 eV, 461 nm) and H3 (see Fig. 2 (a)) were observed. The weak bands of the NV defect are observed only at liquid nitrogen cooling.

It should be noted that the N3a system is caused by the N_3V defect embedded in "platelets" – lamellar agglomeration of interstitials [14]. This system is difficult to reproduce in the laboratory, so it is important for the identification of natural diamonds.

In the PL spectra of the CN4 sample, even at room temperature, clearly recorded ZPL of the NV^0 defect was observed both in the case of excitation in the fundamental absorption region and in the region of extrinsic absorption (see Fig. 2 (b)). It is possible that in this sample NV defects were formed as a result of the dissociation of nitrogen defects of a higher order (N_2V, N_3V, etc.) as a result of high-temperature annealing.

The study of the impurity-defect composition of natural and HPHT diamonds and its transformation under the action of radiation-thermal treatment as applied to NV-defects will enable to use natural raw materials for the production of lasers in the visible range.
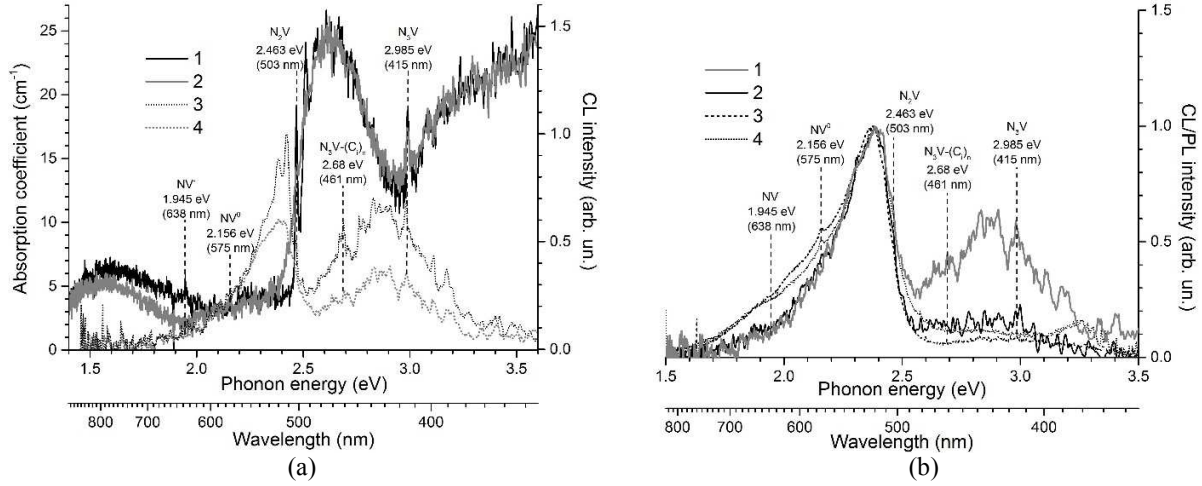
FIGURE 2. Absorption, cathodoluminescence and photoluminescence spectra of a natural sample CN4 subjected to radiation-thermal treatment. a) Absorption spectra (curves 1 and 2) and cathodoluminescence (curves 3 and 4) when cooled with liquid nitrogen (curves 1 and 3) and at room temperature (curves 2 and 4). b) Spectra of cathodoluminescence (curves 1 and 2) and photoluminescence (curves 3 and 4) at room temperature. Curve 1 – the CL spectrum under excitation by an electron beam with a duration of 0.1 ns, curve 2 – the CL spectrum, a beam of 2 ns, curve 3 – the PL spectrum under excitation by an excilamp at 222 nm, curve 4 – the PL spectrum, excilamp 308 nm.

CHERENKOV RADIATION IN DIAMOND

In TOKAMAK-type installations, registration of runaway electrons is produced by ChR detectors, including those based on diamond [4]. The ChR spectrum in diamond during deceleration of the electron beam can be calculated by the formula:

$$I = \frac{4\pi^2 e^2 V}{\lambda^3} \cdot \left(1 - \frac{c^2}{V^2 n^2}\right), \tag{3}$$

where n is the refraction index of diamond, λ is the ChR wavelength, V is the electron beam velocity, c is the speed of light in vacuum. The energy threshold for ChR observing depends on the refractive index of the medium. The magnitude of the velocity (energy) of the electrons for which the expression in brackets equals zero in formula (3) is the threshold. For $n = 2.42$, the threshold energy of ChR observation is ~ 50 keV.

In Fig. 3, the solid curve denotes the ChR spectrum in diamond, calculated by formula (3). The squares and circles represent the CL spectra of natural (C4) and CVD (C5) samples, respectively, under the action of runaway electrons with an energy maximum of 80–100 keV. The spectra were measured at room temperature using a monochromator and a photomultiplier. The values in the spectra are the integrals of the pulses of a photomultiplier. The long-wavelength part of the spectra is due to the CL of the samples, and the short-wavelength part – to the ChR.
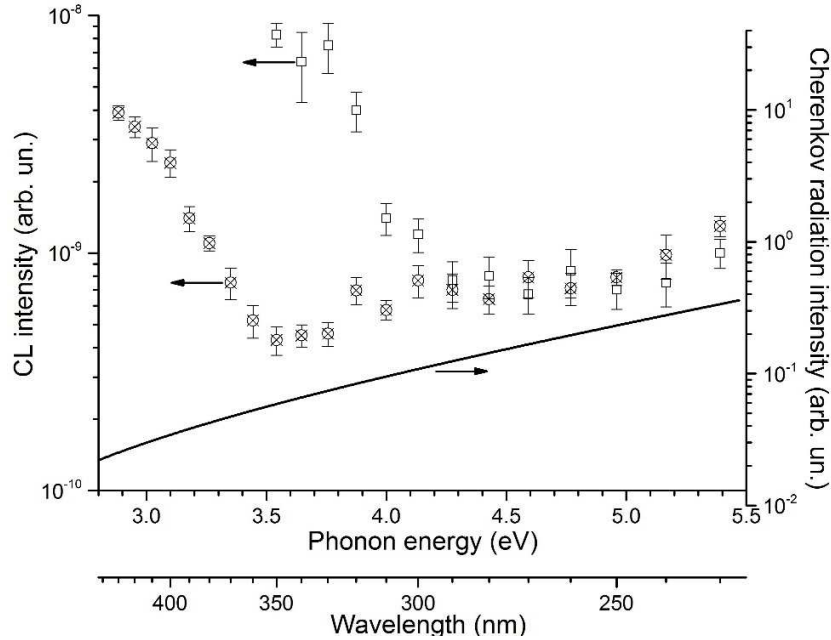
FIGURE 3. Cathodoluminescence spectra of natural IIa sample C4 (squares) and synthetic CVD sample C5 (circles) when excited by a 100-ps runaway electron beam. The solid curve is the calculated Cherenkov-Vavilov radiation spectrum for an 80–100 keV runaway electron beam with duration of 100 ps.

Thus, when measuring ChR, it is necessary to select diamond samples that are transparent up to the fundamental edge, but at the same time weakly luminescent. At the same time, the heating of the detectors above 500 °C as a result of being close to the TOKAMAK core minimizes the CL effect.

SPLITTED STATE OF FREE EXCITONS IN DIAMOND

The PL spectra of a pure CVD sample C10 when excited by laser radiation at 222.2 nm with an intensity of 7, 10, and 13 MW/cm^2 are shown in Fig. 4 (a) [15]. At an intensity of 7 MW/cm^2, the recombination emission band of free excitons (FEs) is observed in the PL spectrum in the form of two one-phonon (TO and TA, 5.272 and 5.323 eV, 235.2 and 232.9 nm) and one two-phonon (TO+OΓ, 5.115 eV, 242.4 nm) component. The phonon components LO and LA are indistinguishable due to their low intensity.

An increase in intensity at low temperatures (less than 200 K) leads to the appearance in the PL spectrum of an additional band of radiative recombination of EHL droplets in the form of two broad components at 5.219 and 5.067 eV (237.5 and 244.7 nm).

An increase in the intensity at high temperatures leads to the broadening of the long-wavelength shoulders of the phonon components of the FE band, which cannot be explained within the framework of thermal broadening. It was previously assumed that this broadening is associated with the plasma band of electron-hole pairs [16]. We suppose that it can be explained by an increase in the population of high-energy sublevels of the FE split state with increasing temperature.
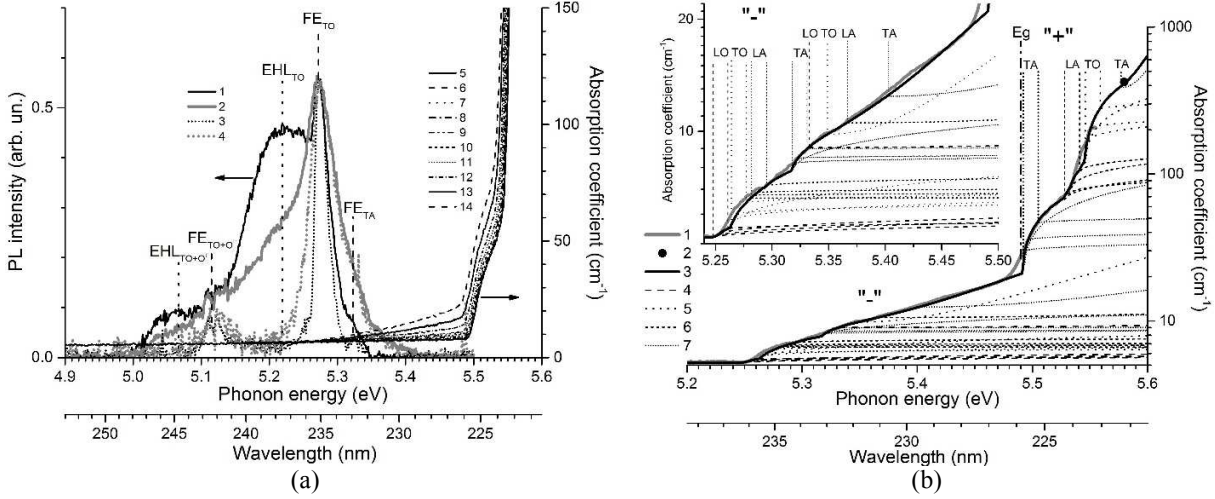
FIGURE 4. a) Photoluminescence spectra of the pure CVD sample C10 when excited at 222 nm with a peak intensity of 13 MW/cm^2 (curves 1 and 2) and 7 MW/cm^2 (curves 3 and 4) when cooled with liquid nitrogen (curves 1 and 3) and room temperature (curves 2 and 4); optical absorption spectra of a HPHT sample C12 near the fundamental edge at temperatures of 83 K – curve 5, 103 K – 6, 123 K – 7, 152 K – 8, 177 K – 9, 202 K – 10, 227 K – 11, 248 K – 12, 273 K – 13, 299 K – 14. b) Absorption spectrum of a HPHTsample C12 near the fundamental edge at 299 K – curve 1, absorption value of the sample C12 at a wavelength of 222.2 nm [17] – 2, approximation of absorption spectrum using formula (5) – 3, the contribution of the phonon modes LO, TO, LA and TA – 4, 5, 6 and 7, Eg - the band gap (5.49 eV), "–" and "+" – "negative" and "positive" absorbing branches.

We attempted to decompose the obtained spectra into components, but so far we have not obtained good agreement with the experiment. Note that the position of the TO component almost does not shift when measuring temperature from 81 to 298 K. It is known that with increasing temperature, the band gap of a semiconductor decreases due to an increase in interatomic distances. Those with increasing temperature, the position of TO component should shift to the long-wave side according to the formula:

$$h\nu = Eg - Ex_i - h\omega_p,$$ (4)

where $h\nu$ is the energy of the emitted photon, Eg is the energy gap, Ex_i is the i-th sublevel of the FE split state, $h\omega_p$ is the phonon energy of the corresponding mode. However, the shift of the maxima of the recombination radiation is not observed. In our opinion, as the temperature rises, the high-energy sublevels of the FE state populate. Thus, two trends level each other.

It is more convenient to observe the fine splitting of the FE state in the optical absorption spectra (OA) near the fundamental edge. Figure 4 (a) (right scale) shows the set of the OA spectra of the HPHT sample C12 in the temperature range 83–299 K [17]. Note that in the region of > 5.25 eV (< 236 nm), in diamond a strong dependence of the OA spectrum on temperature is observed. Moreover, at temperatures less than 177 K, the OA spectrum practically does not change with temperature. At high temperatures, a sharp increase in the absorption occurs in the region > 5.25 eV with increasing temperature to room temperature.

The absorption spectrum of diamond near the fundamental edge is described by the formula [18]:

$$\alpha = \sum_p \left(\frac{n_B + 0.5 \pm 0.5}{h\nu} \cdot \sum_i [A_{p,i}(h\nu - (Eg - Ex_i \pm h\omega_p))^{1/2} + B_p(h\nu - (Eg \pm h\omega_p))^2] \right),$$ (5)

where $n_B = \left(e^{h\omega/k_B T} - 1 \right)^{-1}$ is the phonon energy distribution of Bose-Einstein; "–" in the symbol "±" means

"negative" branch of absorption, i.e. photon absorption with phonon absorption; "+" in the "±" symbol means the "positive" branch of absorption, i.e. photon absorption with phonon emission; subscript p denotes phonon modes (TA, LA, TO, LO); subscript i – sublevels of the FE split state; $A_{p,i}$ are the elements of the transition matrix for the i-th sublevel for various phonon modes p; B_p is the element of the interband transition matrix for various phonon

modes p; Eg is the band gap; Ex_i is the binding energy for the i-th sublevel of the FE state; $h\omega_p$ is the phonon energy of the corresponding phonon mode; k_B is the Boltzmann constant; T is the temperature.

In [19], the splitting of the FE state was explained by the cumulative effect of exchange and spin-orbit interactions and mass anisotropy. In this case, 4 sublevels of the FE state were observed in the PL spectra.

Figure 4 (b) shows the result of approximation of the OA spectrum of sample C12 using formula (5). We used the following values: $Eg = 5.49$ eV, $h\omega_{TA} = 87$ meV, $h\omega_{LA} = 123$ meV, $h\omega_{TO} = 141$ meV, $h\omega_{LO} = 157$ meV, $h\omega_{O\Gamma} = 165$ meV, $Ex_1 = 85.3$ meV, $Ex_2 = 82.2$ meV, $Ex_3 = 79.3$ meV, $Ex_4 = 71.9$ meV. The elements of the $A_{p,i}$ and B_p transition matrices acted as fitting parameters.

It is obvious that 4 sublevels of the FE state are not enough to approximate the fundamental edge of absorption. According to the theory [19], the FE state is split into at least 12 sublevels. Perhaps only 4 of them are optically bright, or previously the spectral resolution was not sufficient to observe all the sublevels.

We plan to study in details the fine splitting of the FE state for a better understanding of the observed phenomena, in particular, the radiative recombination of the FE and the EHL in diamond.

CONCLUSION

Radiation destruction in diamond is manifested in the form of vibronic systems of vacancies (GR1) and interstitials (3H). The GR1 system is well observed in the absorption spectra at concentrations of neutral vacancies above 10^{17} cm^{-3}. The 3H system is observed in the luminescence spectra of pure samples at much lower concentrations.

The charge state of the NV centers depends on the impurity-defect composition of the sample, i.e. from the position of the Fermi level in the band gap of the diamond. To create NV defects in natural diamonds in a negative charge state, it is necessary to use samples with a low degree of nitrogen aggregation.

Accelerated particles during deceleration in diamond lose their energy, including the Cherenkov radiation. At room temperature, observation of ChR is hampered by the cathodoluminescence.

The fine splitting of the free excitons state is accompanied by the temperature dependence of the population of the FE split sublevels, which affects the absorption spectra to the state of free excitons and the luminescence spectra in the recombination bands of free excitons and the electron-hole liquid.

ACKNOWLEDGMENTS

REFERENCES

1. D. V. Prosvirin, V. N. Amosov, A. V. Krasil'nikov, N. M. Gvozdeva, Prib. Tekh. Eksp. **5**, 113–116 (2004) [Instrum. Exp. Tech. **47** (5), 675–677 (2004)].
2. V. S. Feshchenko, A. A. Altukhov, S. A. Lvov, V. A. Shepelev, A. Yu. Mityagin, Datchiki & Systemi (Sensors & Systems) **2**, 37–40 (2011).
3. V. V. Plyusnin, L. Jakubowski, J. Zebrowski, H. Fernandes, C. Silva, K. Malinowski, P. Duarte, M. Rabinski, and M.J. Sadowski, Rev. Sci. Instrum. **79** (10), 10F505 (2008).
4. D. A. Sorokin, A. G. Burachenko, D. V. Beloplotov, V. F. Tarasenko, E. Kh. Baksht, E. I. Lipatov, and M. I. Lomaev, J. Appl. Phys. **122**, 154902 (2017).
5. I. Romet, E. Aleksanyan, M. G. Brik, G. Corradi, A. Kotlov, V. Nagirnyi, K. Polgár, J. Lumin. **177**, 9–16 (2016).
6. E. I. Lipatov, K. R. Burumbayeva, D. E. Genin, V. S. Ripenko, M. A. Shulepov, V. F. Tarasenko, Proc. SPIE **10614**, 106141H (2018).
7. E. I. Lipatov, A. G. Burachenko, V. F. Tarasenko, M. A. Bublik, N. E. Khoroshman, Proc. SPIE **10614**, 106140I (2018).
8. K. Thonke, R. Schliesing, N. Teofilov, H. Zacharias, R. Sauer, A. M. Zaitsev, H. Kanda, T. R. Anthony, Diam. Relat. Mater. **9**, 428–431 (2000).
9. R. Shimano, M. Nagai, K. Horiuch, M. Kuwata-Gonokami, Phys. Rev. Lett. **88**, 057404 (2002).
10. E. I. Lipatov, D. E. Genin, V. F. Tarasenko, Pis'ma v Zh. Eksper. Teoret. Fiz. **103** (11), 755–761 (2016) [JETP Lett. **103** (11), 663–668 (2016)].

11. J. Wrachtrup, S. Ya. Kilin, A. P. Nizovtsev, Opt. Spektrosk. **91** (3), 459–466 (2001) [Opt. Spectrosc. **91** (3), 429–437 (2001)].
12. A. M. Zaitsev, *Optical Properties of Diamond: A Data Handbook* (Springer, Berlin, 2001).
13. G. Davies, M. F. Thomaz, M. H. Nazare, M. M. Martin, and D. Shaw, J. Phys. C: Solid State Phys. **20**, L13 (1987).
14. E. I. Lipatov, A. G. Burachenko, S.M. Avdeev, V. F. Tarasenko, M. A. Bublik, Izv. Vyssh. Uchebn. Zaved., Fiz. **61** (3), 62–75 (2018) [Russ. Phys. J. **61** (3), 469–483 (2018)].
15. E. I. Lipatov, D. E. Genin, D. V. Grigor'ev, V. F. Tarasenko, Izv. Vyssh. Uchebn. Zaved., Fiz. **59** (9-2), 131–135 (2016).
16. Y. Sakamoto, K. Murayama, Y. Nishioka, H. Okushi, Diam. Relat. Mater. **18**, 759–763 (2009).
17. E. I. Lipatov, D. E. Genin, V. F. Tarasenko, Opt. Spektrosk. **119** (6), 902–908 (2015) [Opt. Spectrosc. **119** (6), 918–923 (2015)].
18. P. Grivickas, V. Grivickas, J. Linnros, A. Galeckas, J. Appl. Phys. **101**, 123521 (2007).
19. Y. Hazama, N. Naka, H. Stolz, Phys. Rev. B **90**, 045209 (2014).